

AD-A135 717

PRELIMINARY STUDY FOR THE MODELING OF AN ARTIFICIAL
ICING CLOUD(U) CALIFORNIA STATE UNIV NORTHRIDGE SCHOOL
OF ENGINEERING AND CO. . M EPSTEIN ET AL. AUG 83

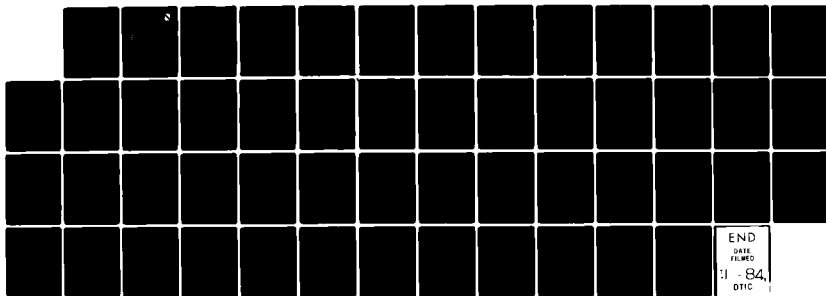
1/1

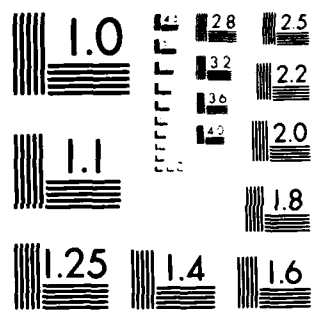
UNCLASSIFIED

AFTC-TIM-83-4 F04700-83-M-0054

F/G 4/1

NL



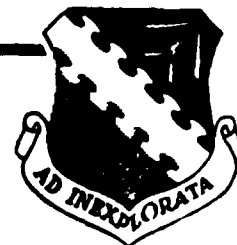


MICROCOPY RESOLUTION TEST CHART
NATIONAL BUREAU OF STANDARDS-1963-A

DTIC FILE COPY

AD-A135717
A
F
F
I
C

AFFTC-TIM-83-4



**PRELIMINARY STUDY for the MODELING
of an ARTIFICIAL ICING CLOUD**

Melvin Epstein

Slamak Moini

G. Thielman

John Vilja

School of Engineering and Computer Science

California State University Northridge

**FINAL REPORT
AUGUST 1983**

DEC 14 1983

**This document has been approved
for public resale and release.
Its distribution is unlimited.**

**AIR FORCE FLIGHT TEST CENTER
EDWARDS AIR FORCE BASE, CALIFORNIA
AIR FORCE SYSTEMS COMMAND
UNITED STATES AIR FORCE**

83 12 13 061

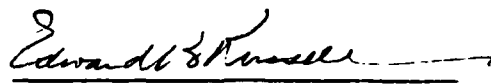
This report was submitted by the School of Engineering and Computer Science, California State University, Northridge, 18111 Nordhoff Ave, Northridge, CA 91330, under Contract No. F0470083M0054, Job Order Number SC6320, with the Air Force Flight Test Center, Edwards AFB, California 93523. Mr B. Lyle Schofield was the AFFTC Project Engineer in charge of the procurement.

This report has been reviewed and cleared for open publication and/or public release by the AFFTC Office of Information in accordance with AFR 190-17 and DODD 5230.0. There is no objection to unlimited distribution of this report to the public at large, or by DTIC to the National Technical Information Service (NTIS). At NTIS it will be available to the general public including foreign nationals.

Publication of this report does not constitute Air Force approval of its findings or conclusions. It is published only as a record of the technical effort.

This report has been reviewed
and is approved for publication:


Mel Epstein
Faculty Advisor


EDWARD B. RUSSELL, Colonel, USAF
Commander, 6520 Test Group

When U. S. Government drawings, specifications, or other data are used for any purpose other than a definitely related government procurement operation, the government thereby incurs no responsibility nor any obligation whatsoever; and the fact that the government may have formulated, furnished, or in any way supplied the said drawings, specifications, or other data is not to be regarded by implication or otherwise, as in any manner licensing the holder or any other person or corporation, or conveying any rights or permission to manufacture, use, or sell any patented invention that may in any way be related thereto.

Do not return this copy; retain or destroy.

UNCLASSIFIED

SECURITY CLASSIFICATION OF THIS PAGE (When Data Entered)

REPORT DOCUMENTATION PAGE		READ INSTRUCTIONS BEFORE COMPLETING FORM
1. REPORT NUMBER AFFTC-TIM-83-4	2. GOVT ACCESSION NO. AD A135 717	3. RECIPIENT'S CATALOG NUMBER
4. TITLE (and Subtitle) Preliminary Study for the Modeling of an Artificial Icing Cloud		5. TYPE OF REPORT & PERIOD COVERED Final Report Oct 82 - Aug 83
		6. PERFORMING ORG. REPORT NUMBER
7. AUTHOR(s) Melvin Epstein John Vilja Siamak Moini G. Thielman		8. CONTRACT OR GRANT NUMBER(s) F0470083M0054
9. PERFORMING ORGANIZATION NAME AND ADDRESS School of Engineering and Computer Science California State University, Northridge		10. PROGRAM ELEMENT, PROJECT, TASK AREA & WORK UNIT NUMBERS
11. CONTROLLING OFFICE NAME AND ADDRESS 6520 TESTG/ENMT, Stop 239 Edwards AFB, CA 93523		12. REPORT DATE August 1983
		13. NUMBER OF PAGES 45
14. MONITORING AGENCY NAME & ADDRESS (if different from Controlling Office)		15. SECURITY CLASS. (of this report) UNCLASSIFIED
		15a. DECLASSIFICATION/DOWNGRADING SCHEDULE
16. DISTRIBUTION STATEMENT (of this Report) This document as been approved for public release and resale. Its distribution is unlimited.		
17. DISTRIBUTION STATEMENT (of the abstract entered in Block 20, if different from Report)		
18. SUPPLEMENTARY NOTES		
19. KEY WORDS (Continue on reverse side if necessary and identify by block number) Cloud Icing Fluid		
20. ABSTRACT (Continue on reverse side if necessary and identify by block number) An evaluation was made of the essential features required to generate an effective model of an artificial icing cloud. Several alternatives were considered. A turbulent mixing length/integral method approach appears to be the most promising. A preliminary version of the fluid mechanical aspects of this model was developed and found to predict overall cloud sizes comparable to those observed during flight tests. Calculations of the radial velocity distributions in the cloud suggest that radial stratification of droplets according to size may occur (large droplets near the periphery and small droplets near the center).		

DD FORM 1 JAN 73 1473

EDITION OF 1 NOV 65 IS OBSOLETE

UNCLASSIFIED

SECURITY CLASSIFICATION OF THIS PAGE (When Data Entered)

UNCLASSIFIED

SECURITY CLASSIFICATION OF THIS PAGE(When Data Entered)

20. (Continued)

Recommendations for future work are included.

UNCLASSIFIED

SECURITY CLASSIFICATION OF THIS PAGE(When Data Entered)

TABLE OF CONTENTS

	<u>Page No.</u>
ABSTRACT	2
LIST OF FIGURES	3
LIST OF SYMBOLS	4
INTRODUCTION	7
ANALYSIS	11
GENERAL CONSIDERATIONS	11
ALTERNATIVE MODELING APPROACHES	15
PRELIMINARY FORM OF THE FLOW MODEL	18
ADDITIONAL CONSIDERATIONS REGARDING THE PROPOSED MODEL	24
MASS, MOMENTUM AND ENERGY EXCHANGE	27
CONCLUSIONS	31
RECOMMENDATIONS FOR FUTURE WORK	33
APPENDIX - NONDIMENSIONAL PARAMETERS	35
REFERENCES	38



A-1

ABSTRACT

An evaluation was made of the essential features required to generate an effective model of an artificial icing cloud. Several alternatives were considered. A turbulent mixing length/integral method approach appears to be the most promising. A preliminary version of the fluid mechanical aspects of this model was developed and found to predict overall cloud sizes comparable to those observed during flight tests. Calculations of the radial velocity distributions in the cloud suggest that radial stratification of droplets according to size may occur (large droplets near the periphery and small droplets near the center). Recommendations for future work are included.

LIST OF FIGURES

<u>Figure No.</u>	<u>Title</u>	<u>Page No.</u>
1	Classical Wake Analysis	41
2	Nondimensional Axial Velocity Profiles	42
3	Variation of Axial Velocity Defect with Axial Distance	43
4	Variation of Cloud Radius with Axial Distance	44
5	Variation of Cloud Radius with Axial Distance	45
6	Radial Velocity Profile	46
7	Improved Velocity Profiles	47
8	Droplet Size Distribution	48

LIST OF SYMBOLS

A	area
A, B, C, D	constants defined by eq. 33
a, b	constants defined by eq. 17
C_D	drag coefficient
C_p, C_v	specific heats
F	force, or function defined by eq. 35
h	heat transfer coefficient
h_v	latent heat of vaporization
k_x	mass transfer coefficient
\bar{M}	molecular weight
\dot{m}	mass flow rate
R	cloud radius
Re	Reynolds number
r	radial distance
Sc	Schmidt number
s	distance along cloud boundary
T	temperature
t	time
u	axial velocity component
V	nondimensional velocity defect, or velocity
v	radial velocity component
W	nondimensional radial velocity component
x	axial distance, or mass fraction
α	entrainment coefficient
β	velocity profile parameter

η	nondimensional radial distance
μ	viscosity coefficient
ξ	nondimensional axial distance
ρ	mass density

subscripts

B	base
d	droplet
s	saturation conditions
v	vapor
w	water
0	centerline value, or initial condition
1	deficit
∞	free stream

THIS PAGE INTENTIONALLY LEFT BLANK

INTRODUCTION

During the last several years the Icing Test and Development Group at the Air Force Flight Test Center has been developing an innovative in-flight experimental technique for evaluating aircraft icing problems. This technique involves the production of a cloud of supercooled water droplets extending several hundred feet behind a tanker aircraft. The cloud, several feet in diameter, is produced by injecting water through spray nozzles arranged in an array suspended below and aft of the tanker aircraft. A test aircraft is maneuvered into an appropriate position behind the tanker so as to immerse a portion of the aircraft in the icing cloud. Observations are made of the buildup and shedding of ice on the immersed surfaces.

Although icing clouds have been produced in this fashion and buildup and shedding of ice on aircraft surfaces have been observed, it is not clear that the cloud properties correctly simulate the icing environment in natural clouds. It is considered especially important that the droplet size distribution in the artificial cloud correspond as closely as possible to that observed in natural icing clouds.

The droplet size distribution in the test region of the cloud depends on a large number of parameters including the details of the spray nozzle design, the geometric arrangement of the array of spray nozzles, the altitude and speed of the tanker, ambient atmospheric conditions and the details of the flow field generated behind the spray nozzle array.

Since a complete experimental simulation of all of these factors in a ground based facility cannot be achieved, a theoretical model which would characterize the essential features of an artificial icing cloud would be very useful.

A survey of the literature on this subject has uncovered only a few attempts to model the development of a droplet cloud produced by an array of spray nozzles. The earliest pertinent work appears to be a model developed by Shapiro, et al (Ref. 1).

Although their analysis was strictly one-dimensional and allowed for only uniform droplet sizes, their modeling of the mass, momentum and energy exchanges was fairly complete. Several years later, Hoffman developed a similar one-dimensional model (Ref. 2). His model was more general in that it allowed consideration of both liquid and solid particles. On the other hand, he didn't allow for any phase change and was therefore unable to account for changes in drop size due to evaporation. A decade later Willbank and Schulz (Ref.3) published a report that included a very detailed treatment of the mass, momentum and energy interchange and was also applicable to nonuniform droplet size distributions. However, their work was also strictly one-dimensional. In a more recent paper, Miller (Ref.4) focused on the question of the freezing out of supercooled droplets but concluded that the required data was unavailable to perform calculations. Since no comparison between any of these models and experimental data has been found, the validity of these models has yet to be assessed.

Furthermore, in all of these studies the flow fields were taken to be strictly one-dimensional. Although some important progress has been made in modeling the mass, momentum and energy interchanges between the liquid and gas phases, no significant work appears to have been done on the modeling of the free expansion of the cloud and its effect on the droplet properties. That expansion has a two-fold effect. It importantly alters the mass, momentum and energy interchange between the phases (and hence the droplet properties in the test region). It also provides a flow velocity normal to the axis of the cloud which (a) increases the cloud diameter, and (b) provides a mechanism for stratifying the droplet size distribution in the cloud both horizontally and radially.

There is clearly a lack of a suitable model to describe the physical characteristics of an icing cloud generated in flight. This report describes a study undertaken to suggest an effective approach to developing such a model.

This study includes:

- (a) an examination of the possibility of correlating existing experimental data using an appropriate set of nondimensional parameters (see Appendix);
- (b) an evaluation of existing models of mass, momentum and energy exchange between phases;
- (c) considerations regarding alternative cloud modeling approaches (including the selection of a preferred approach);
- (d) additional studies conducted to lay the groundwork for future work on the recommended model.

Recommendations for future work are included at the end of the report.

THIS PAGE INTENTIONALLY LEFT BLANK

ANALYSIS

A. General Considerations

An examination of photographs, motion picture film and available experimental data indicates that the icing cloud consists of a freely expanding volume of air, water vapor and water droplets trailing behind the spray nozzle array. The primary features of interest are: (a) the physical extent of the cloud and the air velocity distribution within it, and (b) the characterization of the droplet size, number, velocity, and temperature distribution within the cloud. In principle, these two facets of the cloud are coupled. However, the results of the previous one-dimensional cloud model studies indicate that the air flow properties within the cloud are only slightly dependent on the details of the droplet histories. On the other hand, the droplet histories are strongly dependent on the air velocity distribution within the cloud (see especially Ref. 3). To put this another way, the droplets develop within the aerodynamic flow field generated by the array, but the presence of the droplets play only a secondary role in determining the overall character of the aerodynamic flow field.

Accordingly, any model should provide an appropriate description of the aerodynamic flow field inside of which the droplets evolve in accordance with prescribed rules for the exchange of mass, momentum and energy between the liquid and gas phases.

The essential feature of the developing aerodynamic flow field behind a practical in-flight array is the free turbulent mixing between the injected fluids and the air flowing through and around the array. In the absence of fluid injection, the spray nozzle array produces a wake within which the flow velocities are smaller than the free stream value. The conventional Eulerian frame of reference is adopted in this report in which all velocities are

measured with respect to the array. In this frame of reference the mean flow field is steady. Since the average velocities of liquid and air exiting the spray nozzles are smaller than the flight velocity, the cloud will maintain its wake-like character.

The classical theory of wake flows deals primarily with the wakes behind solid bodies. Very simple and accurate equations are available for the far wake - that is, the region far behind the body producing the wake (Ref. 5). The theory for the near wake (i.e., between the base of the body and the far wake) is in a much less satisfactory state. This is primarily due to the existence of large recirculating regions immediately behind the base of a solid body. Such recirculating regions may be expected to be quite small behind the open spray nozzle arrays characteristic of the present problem. Although the calculation of this type of near wake should be much easier than for that behind a solid body, no such theory is available in the literature. Any icing cloud model will have to address this problem.

Before alternative models of the icing cloud are described, a brief digression regarding the far wake is in order. The classical (i.e., no injection) far wake analysis is based on the observation that there is a region of decreased velocity in the wake behind the body (Fig. 1). If u_0 is the axial speed of the flow on the axis and u_∞ is the free stream speed, then one can define an axial velocity deficit by

$$u_i = u_\infty - u_0 \quad (1)$$

As a result of this velocity deficit, there is a corresponding axial momentum deficit relative to the free stream momentum flux approaching the body. According to the principle of conservation of momentum, since there is no force on the fluid downstream of the base, the total momentum defect in the wake is independent of the axial location, x , and is equal to the drag of the

body that produced the wake. I.e.,

$$2\pi \int_0^{R(x)} \rho u (u_\infty - u) r dr = \text{Drag} = \frac{1}{2} \rho u_\infty^2 A_B C_D \quad (2)$$

where ρ is the free stream density, $R(x)$ is the local wake radius, r is the radial distance from the axis of the wake, C_D is the drag coefficient of the body and A_B is the base area of the body. For a circular cross section

$$A_B = \pi R_B^2 \quad (3)$$

where R_B is the radius of the base. As turbulent mixing takes place, the velocity deficit on the axis decreases and the wake radius increases such that the integral in eq. 2 remains constant.

It can be shown that sufficiently far downstream of the base of the body (the far wake) the wake radius and velocity deficit in the wake are given by

$$R(x) = \left(\frac{3\beta R_B^2 C_D}{2} x \right)^{1/3} \quad (4)$$

$$\frac{u_1}{u_\infty} = \left(\frac{R_B C_D^{1/2}}{3\sqrt{2} \beta x} \right)^{2/3} \quad (5)$$

where β is a turbulent mixing coefficient.

The same approach can be used to determine the asymptotic (i.e., far wake) solution when there is injection. It is instructive to do this in two steps.

First, consider pure air injection. Again, since there is no external force acting on the fluid downstream of the point of injection, the total momentum in the wake must remain constant. However, in this case the initial momentum is increased by the momentum of the injected air. The latter can be shown to be equal to the thrust produced by the nozzles injecting the air. Consequently eqs. 2, 4 and 5 still apply provided the drag is replaced by the drag minus the thrust and C_D is replaced by an effective drag coefficient

defined by

$$\text{Drag} - \text{Thrust} = \frac{1}{2} \rho u_a^2 A_B C_D' \quad (6)$$

A similar argument can be made when water injection is added. However, in that case the water must be treated as a separate fluid. The relative velocity between air and water droplets accelerates the droplets to the local airspeed some distance downstream of the point of injection. According to Newton's third law, the force of the air on the droplets is equal and opposite to the force of the droplets on the air. According to Newton's second law, this produces a reduction in the momentum flux of the air. If the rate of mass addition due to water injection is \dot{m}_w and the injection velocity is characterized by u_{w_0} , then by the time the droplets reach the far wake, the momentum transfer is $\dot{m}_w(u_a - u_{w_0})$. Eqs. 4 and 5 still apply provided the effective drag coefficient is further modified as follows

$$\text{Drag} - \text{Thrust} + \dot{m}_w(u_a - u_{w_0}) = \frac{1}{2} \rho u_a^2 A_B C_D'' \quad (7)$$

This modified far wake analysis provides a very simple tool for estimating the effects of the array geometry and fluid injection parameters on the size of the cloud that is generated. For example, eq. 4 shows that the cloud radius can be increased by increasing the size of the array and/or the effective drag coefficient. From eq. 7 it can be seen that the effective drag coefficient can be increased by

- a) using an array with a higher drag coefficient
- b) reducing the thrust of the injected fluid. This can be achieved by reducing the air injection velocity but more effectively by injecting in the upstream direction so that the nozzles produce drag rather than thrust.
- c) increasing the momentum exchange between the air and the droplets. This

can be achieved by injecting either laterally or upstream rather than downstream.

These results are very useful for predicting the overall size and shape of the icing cloud but provide virtually no information about the droplet properties in the cloud. A much more detailed model of the cloud is required for that purpose. Considerations regarding the selection of an appropriate modeling approach is provided in the next section.

B. Alternative Modeling Approaches

From the previous discussion it is clear that the modeling approach to be chosen should be capable of describing the development of a wake-like region with air and water injection at the upstream end of the wake. Furthermore, it must be capable of accounting for the exchange of mass, momentum and energy between the water droplets, the water vapor and the air entrained in the wake. Fortunately, the mass, momentum and energy exchanges at a point depend only on the local properties of the flow field.

The modeling of those effects appear to have been adequately treated in the strictly one-dimensional models referenced in an earlier section. A discussion of that part of the problem will be presented in a later section of this report.

The primary new feature that needs to be modeled is the development of a freely expanding cloud with internal phase change and mass, momentum and energy exchange. It was pointed out in the last section that the freely expanding cloud is essentially a constant pressure, turbulent wake. Unfortunately, not enough is known about turbulent mixing to allow a detailed prediction of the turbulent flow field, even without the complication of liquid injection. However, some approximate techniques developed for other applications offer the promise of being able to predict the mean flow property distributions in the wake.

There are three general approaches which might be considered.

1) Two-dimensional finite difference calculations. This is the most detailed and sophisticated approach in which the complete system of partial differential equations are integrated numerically. These equations include a turbulence transport equation which models the local turbulent mixing. Although success has been had with some problems using this approach, its value for this application is problematical because:

- a) it is complicated to formulate and program and requires considerable execution time on the computer.
- b) the effects of the water droplets on the turbulent transport equation are unknown. The development of a dependable model would be a research project in itself.
- c) the uncertainties in the characterization of the properties of the injected fluid entering the wake would appear to make the undertaking of such a large computational task cost ineffective.

2) Scheduled mixing model. This is a relatively simple model which has been used successfully in a number of jet and wake-like problems involving chemical reactions (Ref. 6). In this approach the rate at which the external flow is entrained in the mixing region is specified a priori. The mixing region is then replaced by a succession of segments within which the flow is treated one-dimensionally. This reduces the partial differential equations to a set of ordinary differential equations. The initial conditions for each segment are determined by using the final conditions from the previous segment and assuming that the fluid at those conditions mixes instantaneously and uniformly with an appropriate amount of the surrounding fluid. By constraining this mixing process to be in accordance with conservation of mass, momentum and energy, the global properties of the flow are correctly determined.

This approach is attractive because of its simplicity and because the phase

change is not unlike a chemical reaction. However, there are two weaknesses to this method which are considered too important to overlook:

- a) the shape of the cloud boundary is too important to be assumed a priori. It is desirable that it be predicted as part of the calculation.
- b) the use of the one-dimensional approximation within each segment may suffice for problems in which only the axial development of the flow properties is of primary importance. It does not give the radial variation of the flow properties. Although the scheduled mixing model could be extended by assuming a priori the shapes of the radial distributions of the flow properties, the approach doesn't appear to offer any advantages over the next method.

3) Integral method. The integral method has a long history of successful applications in viscous flows. In this method, the lateral variations in fluid properties are approximated by simple analytical expressions. These analytical representations are constructed so as to satisfy the boundary conditions and contain a number of undetermined parameters. These analytical formulas are then effectively substituted into the partial differential equations governing the problem and those equations are analytically integrated in the lateral direction. The result is a set of ordinary differential equations for the undetermined parameters. The solution of those equations yields the spatial variation of all flow properties as well as the shape of the boundary of the mixing zone. Since the ordinary differential equations are very much easier to solve numerically than the partial differential equations, the computation is both rapid and cost effective. Furthermore, the simplicity of the equations allows the effects of phase change and mass, momentum and energy exchange to be included without undue complication.

The weakest link in the application of the integral method to turbulent viscous flows has been in finding a simple, yet accurate model of the turbulent mixing process. The traditional mixing length model has sometimes been found to be lacking in accuracy when applied to flows involving solid boundaries. However, it has fared much better when applied to free mixing flows without solid lateral boundaries (Ref. 5). That is precisely the situation that needs to be modeled in the current project.

As a result of these considerations, the integral method is considered to be the most appropriate choice for this problem.

The remainder of this report is devoted to preliminary studies supporting the feasibility of the integral method approach and providing some additional insights into the physical features of icing clouds.

C. Preliminary Form of the Flow Model

The most prominent qualitative feature of a wake flow is that the wake starts off with a nonuniform velocity profile which eventually transforms, through the action of turbulent entrainment, to a uniform profile with $u = u_\infty$ (Fig. 1). For the purposes of illustrating this approach and generating some qualitative information about the cloud, the following preliminary form of the model is presented.

In Ref. 3 it was found that the presence of droplets has a very minor influence on the flow properties of the air. For the present purpose, the injection of water droplets will be neglected. This gives no information about the time history of the droplets (although more will be said about that later in this report). However, it does give a reasonable qualitative picture about the size of the cloud and the velocity distribution therein. It will be seen that this allows certain qualitative features of the droplet behavior in freely expanding clouds to be inferred.

To start, consider a plane normal to the flow (Fig. 1). The rate of mass flow across this plane is

$$\dot{m} = 2\pi \int_0^{R(x)} \rho u r dr \quad (8)$$

The turbulent mixing at the boundary of the cloud entrains air into the cloud. According to the classical turbulent mixing length theory, the rate at which mass flow is entrained into the cloud is

$$d\dot{m} = \alpha \rho (u_0 - u_0) 2\pi R ds \quad (9)$$

where α is the entrainment coefficient, $u_0(x)$ is the velocity on the centerline of the cloud and s is the arc length along the surface of the cloud. Since the cloud grows very slowly, ds may be approximated by dx . More precisely, $ds = dx \sqrt{1 + (dR/dx)^2}$. The latter form will be included in future analyses but its inclusion is not warranted for the present purpose. Differentiating eq. 8 and setting it equal to eq. 9, conservation of mass requires that

$$\alpha R(u_0 - u_0) = \frac{d}{dx} \left[\int_0^{R(x)} u r dr \right] \quad (10)$$

Since there are no external forces acting on the wake, conservation of momentum requires that the momentum defect in the wake remains constant. That is

$$\frac{d}{dx} \left[2\pi \int_0^{R(x)} \rho u (u_0 - u) r dr \right] = 0 \quad (11)$$

Eqs. 10 and 11 are exact. The integral method is introduced by assuming $u(x, r)$ with an appropriate expression which is explicit in r and contains some unknown parameters which are functions of x . Since the qualitative variations of u with r has a cosine-like appearance (Fig. 1), it is assumed in this preliminary form of the model that

$$u = \frac{1}{2} \left[u_0 + u_\infty + (u_0 - u_\infty) \cos \frac{\pi r}{R} \right] \quad (12)$$

where u_0 and R are undetermined functions of x . This form is seen to satisfy the boundary conditions

$$\begin{aligned} u(x, 0) &= u_0(x) \quad , \quad u(x, R) = u_\infty \\ \frac{\partial u}{\partial r} &= 0 \quad \text{at } r=0, R \end{aligned} \quad (13)$$

In order to carry out the rest of the analysis (which can be done without further approximations), it is convenient to introduce the following non-dimensional variables.

$$V = \frac{u_\infty - u_0}{u_\infty} \quad , \quad \eta = \frac{r}{R} \quad (14)$$

Substituting eqs. 12 and 14 into eqs. 10 and 11, performing the integration with respect to r and the differentiation with respect to x yields

$$(1-bV) \frac{dR}{dx} - \frac{bR}{2} \frac{dV}{dx} = \alpha V \quad (15)$$

$$(1-2bV+aV^2) \frac{dR}{dx} - R(b-aV) \frac{dV}{dx} = \alpha V \quad (16)$$

where

$$a = \frac{3}{8} - \frac{2}{\pi^2} \quad , \quad b = a + \frac{1}{8} \quad (17)$$

Equations 15 and 16 can be integrated exactly to yield

$$\frac{R^2}{R_0^2} = \frac{V_0(b-aV_0)}{V(b-aV)} \quad (18)$$

and

$$\begin{aligned} \frac{\alpha x}{R_0} &= \frac{b^2 + 2abV + a(4-8a-b^2)V^2}{b^2 V} \sqrt{\frac{V_0(b-aV_0)}{V(b-aV)}} \\ &\quad - \frac{b^2 + 2abV_0 + a(4-8a-b^2)V_0^2}{b^2 V_0} \end{aligned} \quad (19)$$

where R_0 and V_0 are the initial values of R and V .

It may be noted that V is the nondimensional velocity defect on the centerline. In the far wake the velocity defect disappears (i.e., $V \rightarrow 0$ as $x \rightarrow \infty$). It can be seen from eq. 19 that in the limit as $x \rightarrow \infty$, $V \sim x^{-1/3}$. Since, in that limit, eq. 18 shows that $R \sim V^{-3/2} \sim x^{1/3}$, we see that this solution is consistent with the classical far wake solution presented in eqs. 4 and 5.

The initial values of R and V can be related to the specified mass flow at the nozzle exit plane, the drag of the array and the thrust of the spray nozzles. That is, when the appropriate integrals of the assumed velocity profile (eq. 12) are evaluated at $x=0$, they must give the specified values of mass and momentum flux.

Parametric studies of the cloud flow field were made using these results. The nondimensional form of the velocity profile is shown at various stages of decay in Fig. 2. The variation of centerline axial velocity defect with axial distance is shown in Fig. 3 for various values of V_0 . Note that $V_0=0$ implies zero initial velocity defect and $V_0=1$ implies zero initial centerline velocity. The variation of cloud radius with axial distance is shown in Figs. 4 and 5.

Several features of the cloud may be deduced from these figures. First, we note that the slopes of these curves for large x are in accordance with the classical far wake results. Next, we may note that since the spray nozzle array currently in use has a radius of about two feet and testing is done at a position in the cloud about three hundred feet behind the array, $x/R_0 \approx 150$. Figs. 3 and 4 show that this region is near the beginning of the far wake regime (constant slope on the log-log plots), regardless of the value of the initial momentum defect. In addition, Fig. 4 shows that the cloud radius at this position is about 2 to $2\frac{1}{2}$ times the original radius. This appears to be consistent with in flight photographs of the cloud.

As an aside, it should be noted that the simple cosine variation of velocity

with r is qualitatively reasonable but quantitatively only a first approximation. It is not surprising then that at larger values of V_0 ($\approx .7$), some anomalies develop for small values of x/R_0 (i.e., $x/R_0 < 1$). An improved form for the velocity profile which will better approximate the true velocity profile will be discussed later in this report.

As a point of reference, calculations performed for a test condition of altitude of 18,000 feet, $u = 300$ ft/s and typical water air and injection rates give a value of $V_0 \approx .5$.

Although water injection has not been explicitly included so far one important feature regarding the behavior of water droplets in a freely expanding cloud can be inferred. It had been indicated earlier in this report that all previous models were strictly one-dimensional. In that case all streamlines and droplet trajectories are straight horizontal lines. In a freely expanding cloud however, the streamlines and droplet trajectories are curved. The radial component of the air velocity, v_r , can be determined from the continuity equation in cylindrical coordinates:

$$\frac{\partial(ru)}{\partial x} + \frac{\partial(rv)}{\partial r} = 0 \quad (20)$$

Equation 20 can be integrated formally with respect to r to give

$$v_r = -\frac{1}{r} \int_0^r r \frac{\partial u}{\partial x} dr \quad (21)$$

Substituting eq. 12 into eq. 21 and carrying out the indicated operations provides an analytical expression for v_r . It is convenient to introduce a nondimensional radial velocity defined by

$$W = \frac{v_r}{u_\infty} \quad (22)$$

The result is

$$W = \frac{\alpha V^2}{2\gamma(b-2aV+abV^2)} \left[2(aV-b) \left(\frac{\gamma^2}{2} + \frac{1}{\pi^2} \cos \pi\gamma + \frac{\gamma}{\pi} \sin \pi\gamma - \frac{1}{\pi^2} \right) + (b-2aV) \left(\frac{2\gamma}{\pi} \sin \pi\gamma + \frac{2}{\pi^2} \cos \pi\gamma - \gamma^2 \cos \pi\gamma - \frac{2}{\pi^2} \right) \right] \quad (23)$$

This nondimensional radial component of velocity is plotted versus the nondimensional radial coordinate, η , in Fig. 6. Two important observations are: (a) the radial velocity is inward and peaks at $r/R \approx .5$; and (b) radial velocities approach ten percent of the free stream speed where the axial velocity deficit is large. Droplets injected at the beginning of the cloud will begin their trajectories at the injection angle.

As they move they tend to curve into alignment with the local air velocity vector. Heavier particles will change direction more slowly than lighter particles because of their inertia. In addition, the drag on a droplet depends on its size. More precisely, the force on a droplet is

$$\vec{F} = \frac{1}{2} \rho (\vec{V} - \vec{V}_d)^2 C_{D_d} \pi r_d^2 \quad (24)$$

where \vec{V} is the (dimensional) local air velocity vector, \vec{V}_d is the local droplet velocity vector, C_{D_d} is the droplet drag coefficient and r_d is the droplet radius. For the low Reynolds numbers characteristic of the small droplets, Stokes law gives

$$C_{D_d} = \frac{24\mu}{\rho |\vec{V} - \vec{V}_d| r_d} \quad (25)$$

where μ is the viscosity coefficient for air. Denoting the mass of a droplet by m_d , and substituting eq. 25 into eq. 24, Newton's second law requires

$$m_d \frac{d\vec{V}_d}{dt} = 12\pi\mu r_d |\vec{V} - \vec{V}_d| \quad (26)$$

Since $m_d = (4/3)\pi r_d^3 \rho_w$, eq. 26 can be rewritten as the two scalar equations

$$\frac{du_d}{dt} = \frac{9\mu}{\rho_w r_d^2} (u - u_d) \quad (27)$$

$$\frac{dv_d}{dt} = \frac{9\mu}{\rho_w r_d^2} (v - v_d) \quad (28)$$

where u_d and v_d are the horizontal and radial components of droplet velocity, respectively and ρ_w is the density of water.

The main point of this discussion can be made from eq. 28. It can be seen that the acceleration of the droplets in the radial direction is proportional to r_d^{-2} . This means that a 20 micron droplet experiences 6.25 times the acceleration of a 50 micron droplet. As a result a 20 micron droplet injected

at $\gamma = 1.5$ at a slight positive angle to the axis may quickly align itself with flow and end up closer to the axis. On the other hand, a 50 micron droplet may continue along a diverging trajectory well beyond the test region. In other words, a radial stratification of the droplets will be produced with the larger droplets near the outer boundary of the cloud and the lighter droplets near the axis.

This behavior can be corrected by designing the array to inject a preponderance of smaller droplets near the edge of the cloud and larger ones near the axis. This or other possible solutions to the stratification problem would of course need a cloud model such as the one suggested here to evaluate the proposed solution.

D. Additional Considerations Regarding the Proposed Model

It was pointed out earlier in this report that the cosine velocity distribution velocity profile, although qualitatively correct, cannot be expected to provide accurate quantitative results for all conditions of interest. An alternative form would be an n 'th degree polynomial where n is large enough to represent any real flow of interest.

Given the limitations of turbulent mixing theory and the fact that little detailed information is available regarding the initial velocity profile in the cloud, a very large value of n does not appear to be warranted. In fact, since no data has been found for the initial velocity profile in the cloud there appears to be little justification to use a value of n greater than that needed to assure that all of the boundary conditions are satisfied and that the correct mass and momentum flux into the cloud are accounted for.

The boundary conditions which must be satisfied are

$$\text{at } r=0 \quad u=u_0(x), \quad \frac{\partial u}{\partial r} = 0 \quad (29)$$

$$\text{at } r=R(x) \quad u=u_\infty, \quad \frac{\partial u}{\partial r} = 0 \quad (30)$$

Before describing the mass and momentum fluxes, some reflections on the cosine velocity profile are in order. First note that in eq. 12, the initial

value of u_0 must be specified. This can be accomplished by specifying the entering mass or momentum flux. One of the weaknesses of the cosine velocity distribution is that these fluxes cannot be specified independently. In order to accomplish that goal another undetermined parameter has to be introduced. A suitable polynomial which allows this to be done and satisfies all of the boundary and symmetry conditions is

$$\frac{u}{u_0} = [(1-V) + 3V\eta^2 - 2V\eta^3] [1 + \beta V\eta^2(1-\eta)^2] \quad (31)$$

Specification of the entering mass and momentum fluxes determines the constant β and the initial value of V . This results in a seventh degree polynomial. It is hard to imagine that a higher degree polynomial could be justified given that no detailed knowledge is available regarding the velocity profiles at the nozzle exits.

Parametric calculations have been made to evaluate the kinds of velocity profiles available from eq. 31. Typical results are shown in Fig. 7.

The analysis described in the last section for the cosine velocity profile has been repeated using eq. 31. An exact solution has been obtained for the relation between cloud radius and velocity defect.

$$\frac{R^2}{R_0^2} = \frac{AV_0 + BV_0^2 + CV_0^3 + DV_0^4}{AV + BV^2 + CV^3 + DV^4} \quad (32)$$

where

$$A = .15 - .03333\beta, \quad B = 1.2136 + .56984\beta - .6557\beta^2 \quad (33)$$

$$C = 5.2618\beta + 5.3872\beta^2, \quad D = -5.4210\beta^2$$

The differential equation for $V(x)$ has been reduced to:

$$\frac{dV}{dx} = \frac{\alpha R}{V(dF/dV)} \quad (34)$$

where $R(V)$ is known from eq. 32 and F is given by

$$F(V) = [.5 + (-.15 + .016667\beta)V - .006746]R^2 \quad (35)$$

Eq. 34 can actually be integrated in terms of elliptic integrals but the complexity of the result is not very useful. Future work would involve the numerical integration of the equation.

Most of the discussion thus far has focused on the fluid mechanical aspects of cloud development. The ultimate goal of the cloud model is to determine the properties of the water droplets as they flow back through the cloud.

As the droplets progress through the cloud they (1) accelerate due to the action of the surrounding air, (2) cool off due to thermal conduction and evaporation, and (3) decrease in size due to evaporation. Thus the cloud is actually a mixture of air, water vapor and liquid water droplets. The water droplets interact with the air/vapor mixture through the exchange of mass, momentum and energy. The rates of exchange of these properties depend on the local conditions surrounding each droplet, the size, temperature and speed of each droplet and the exchange coefficients for mass, momentum and energy between phases.

The previous one-dimensional work has indicated that the presence of the water droplets has a very small effect on the properties of the air flow. That is, the droplets behave as though they are in a bath of air and water vapor but the bath is not significantly affected by the presence of the droplets. Preliminary calculations made under this contract indicates that for typical flight conditions this assumption may sometimes be marginal. For the conditions considered in the previous section, the injected air adds about ten percent additional momentum to the cloud. Likewise the momentum transferred to the water droplets from the air is about 20% of the same figure. The net momentum exchange is considered to be just about large enough to warrant inclusion in modeling the aerodynamics of the cloud but not so large as to justify more than a first order refinement of the proposed fluid mechanical model. On the other hand, this momentum exchange is the primary driving force for the dynamics of the droplets. The same qualitative remarks apply with regard to the transfer of mass and energy.

E. Mass, Momentum and Energy Exchange

While the overall fluid dynamic description of the cloud is not expected to be sensitive to the details of the mass, momentum and energy exchange between the phases, it is expected that the droplet properties will depend critically on these mechanisms.

The rates of change of mass, momentum and energy of a spherical drop of liquid have been extensively studied. In applying these results care must be taken that (1) the thermodynamic properties of water near freezing are appropriately accounted for, and that (2) the transfer coefficients are appropriately represented over the Reynolds number range of interest.

A survey of the available data has been undertaken. Very little data has been found on the thermodynamic properties of liquid water and its vapor near freezing temperatures. The data of Ref. 7 are the most complete found to date for the specific heats and heat of vaporization. Refs. 8 and 9 provide data on vapor pressure of the liquid at normal and supercooled conditions, respectively.

Ref. 3 provides the most complete description of the mass, momentum and energy exchange rates which have been found so far. These include

$$\text{mass transfer} \quad \frac{dm_d}{dt} = 4k_x \pi r_d^2 \bar{M}_v \frac{X_v - X_{vs}}{1 - X_{vs}} \quad (36)$$

where m_d is the mass of a droplet, k_x is the mass exchange coefficient, \bar{M}_v is the molecular weight of the vapor, X_v is the mass fraction of the vapor and X_{vs} is the vapor mass fraction at saturation conditions.

$$\text{momentum transfer} \quad m_d \frac{d\bar{V}_d}{dt} = \frac{1}{2} \rho |\bar{V} - \bar{V}_d|^2 \pi r_d^2 C_D \quad (37)$$

where \bar{V}_d and \bar{V} are the droplet and local air velocity vectors, respectively and C_{Dd} is the droplet drag coefficient.

$$\text{energy transfer} \quad m_d C_{vw} \frac{dT_d}{dt} = 4h \pi r_d^2 (T - T_d) + h_v \frac{dm_d}{dt} \quad (38)$$

where C_{vw} is the specific heat at constant volume of water, T and T_d are the local gas and droplet temperatures, respectively, h is the heat transfer coefficient and h_v is the latent heat of vaporization of water.

Suitable low Reynolds number correlations of the transfer coefficients are summarized in Ref. 3 .

$$\text{mass} \quad k_A = \frac{4}{r_d S_c M} (1 + 3 Re^{1/2} S_c^{1/3}) \quad (39)$$

$$\text{momentum} \quad C_{Dd} = \frac{24}{Re} (1 + 15 Re^{.687}) \quad (40)$$

$$\text{energy} \quad h = \frac{\mu C_p}{\rho_g} (1 + 3 Re^{1/2} S_c^{1/3}) \quad (41)$$

where μ is the viscosity coefficient, S_c is the Schmidt number, Re is the Reynolds number of the flow relative to the droplet

$$Re = \frac{\rho(\bar{V} - \bar{V}_d) r_d}{\mu} \quad (42)$$

C_p is the specific heat at constant pressure and Pr is the Prandtl number.

In order to keep computation time as low as possible, a start has been made to consider possible simplifications. For example, the droplet trajectories are governed by eq. 37. Consider the simpler one-dimensional problem.

$$m_d \frac{du_d}{dt} = \frac{1}{2} \rho (u - u_d)^2 \pi r_d^2 C_{Dd} \quad (43)$$

It is of interest to estimate the characteristic relaxation distance for a droplet to attain say 95% of the gas speed. The most conservative estimate is obtained using $U=U_\infty$ and the Stokes relation for C_{Dd} ($C_{Dd}=24/Re$). Since

$m_d = (4/3)\pi r_d^3 \rho_w$, eq. 43 becomes

$$\frac{du_d}{dt} = \frac{9\mu}{\rho_w r_d^2} (u_\infty - u_d) \quad (44)$$

Noting that

$$\frac{du_d}{dt} = u_d \frac{du_d}{dx} \quad (45)$$

and introducing the nondimensional quantities

$$\xi = \frac{x}{r_d}, \quad V_d = \frac{u_d}{u_\infty} \quad (46)$$

eq. 44 becomes

$$V_d \frac{dV_d}{d\xi} = \frac{9}{Re} (1 - V_d) \quad (47)$$

Equation 47 can be integrated easily. Using the most conservative initial condition, $u_d(0) = 0$, one obtains

$$\xi = -\frac{Re}{9} [V_d + \ln(1 - V_d)] \quad (48)$$

For a 50 micron droplet in a 100m/s airstream at 0°C, the droplet reaches 95% of the airstream speed after only 3.3m. Smaller droplets and/or slower airstreams would require smaller distances. This is only about 3% of the distance to the test region. This illustration suggests that this, and perhaps the other transport processes, take place on a time or distance scale short compared to the length of the cloud. The implication is that some sort of quasi-equilibrium approximation may suffice to predict droplet properties at the test location in the cloud. Further work is needed before that hypothesis can be accepted.

Another question which must be addressed is the treatment of the droplet size distribution. It is known that a range of droplet sizes will be injected into the cloud. Since the evaporation and acceleration rates are sensitive to droplet size the model should provide a method to include a given initial droplet size distribution. Preliminary consideration has been given to two possible approaches.

1) The one-dimensional analyses which have treated this aspect of the problem have replaced the actual droplet size distribution by a set of discrete droplet sizes (Fig. 8). In those analyses the flow velocity is independent of the radial coordinate and the calculation is straightforward. In the case of a freely expanding cloud the problem is complicated by the radial variation of flow speed of the air. This can be accounted for by further subdividing each discrete size of droplets into a discrete set of initial radial zones in which the droplets enter the cloud.

2) An alternative approach is to recognize that at a point in the cloud, the change in a droplet's properties will depend on its size, its velocity and the ambient conditions. One can in principle define a droplet distribution function $f(r_d, \bar{V}_d; x, r)$ and a droplet response function $F(r_d, V_d; \text{ambient parameters})$; the latter will give the rate of change of r_d and \bar{V}_d as a function of the ambient parameters. Conceptually, a convolution of these functions will give the spatial variations of droplet properties. In a practical sense, it is expected that this

approach might be useful only if the quasi-equilibrium approximations alluded to above turn out to be justifiable.

CONCLUSIONS

An evaluation has been made of the primary features of a freely expanding icing cloud in order to determine the essential ingredients needed to satisfactorily model the cloud. It has been concluded that the required model must adequately represent (1) a wake-like fluid mechanical flow-field, and (2) the exchange of mass, momentum and energy between the droplets and the surrounding fluid.

None of the previous models for describing the properties of droplets in a flowing gas appears to be applicable to this problem. All previous models are strictly one-dimensional and hence are incapable of describing some of the essential features of a freely expanding cloud. These features include, in addition to the radial variation of the fluid mechanical and droplet properties, an induced stratification of droplet sizes (larger droplets toward the periphery of the cloud, smaller droplets toward the center).

The results obtained from the one-dimensional models show that although the droplet properties depend strongly on their surrounding environment, that environment is not strongly affected by the droplets. There appears to be no reason to reach a different conclusion regarding that one-way coupling for a freely expanding cloud. It would seem then that the droplet mass, momentum and energy exchange can be adequately modelled using the same equations used in the more complete one-dimensional models. However, the properties of the fluid surrounding the droplets must be modelled by a more detailed fluid mechanical model which can appropriately describe the radial variation of the fluid properties.

Several possible approaches were examined. The most promising approach appears to be a turbulent mixing length/integral method approach. A preliminary version of the fluid mechanical part of the model has been developed. The overall size of the cloud predicted by that model appears to be in agreement with in-flight data. As a result of these encouraging observations, development of a refined version of the fluid mechanical part of the model has been initiated.

At the same time studies have been initiated to examine possible simplifications in modelling the mass, momentum and energy exchange between phases.

Perhaps the weakest link in the model is the specification of the properties of the fluids entering the cloud from the array. At the present time it appears that there is not enough data to precisely define the radial distribution of flow properties entering the wake. The proposed model uses a seventh degree velocity profile which matches the global mass and momentum input. This is probably adequate for the fluid dynamic part of the model. It is expected that the accuracy of the model will be limited by the information available on the radial distribution of droplet properties at the upstream end of the cloud.

In this regard, it may be noted that the proposed model is equally applicable to modeling the entire cloud generated by the array, as well as the individual cloudlets generated by each spray nozzle. If detailed information were available on flow and droplet properties at the exit plane of a spray nozzle, the proposed model could be used to model the development of each cloudlet until the individual cloudlets overlapped. The output of that calculation could then be used as the input for the cloud generated by the total array of spray nozzles.

Finally, recommendations are made in the Appendix regarding parameters to be included in experimental measurements which would facilitate the correlation of experimental data.

RECOMMENDATIONS FOR FUTURE WORK

It is recommended that work be continued on the development of the modeling approach described in this report. The suggested order of tasks in this work is:

1. Investigate the possibility of simplifying the mass, momentum and energy exchange equations. Preliminary work suggests that the time scale for change of these properties may be very small compared to the transit time of a fluid particle from the array to the test region. In that case, a quasi-equilibrium hypothesis can be invoked which might drastically simplify the equations. This assessment can be made by performing detailed parametric droplet trajectory calculations for the flow field of the preliminary model described in this report, including the complete description of mass, momentum and energy exchange. The results of such calculations should confirm or deny the validity of the quasi-equilibrium hypothesis.
2. Derive the full equations for the proposed model.
3. Program, debug and execute sample computer calculations for the proposed model
4. Perform parametric calculations for:
 - a) a variety of flight test conditions of interest
 - b) a variety of radial droplet property distributions at the upstream end of the cloud (to determine the sensitivity of the results to uncertainties in the initial conditions).
5. Employ the computer program as a simulation tool to assess the effects of changes in array and spray nozzle design on the effectiveness of the icing cloud.
6. Compare predicted performance with experimental results.

In addition, it is recommended that further work be done, either in a wind tunnel or/and in flight to more completely characterize the initial flow and droplet property profiles at the entrance to the cloud, Similar work should also be done for individual spray nozzles.

APPENDIX

Nondimensional Parameters

A useful way of correlating data from different experiments is to introduce nondimensional parameters. Two approaches were taken to define the nondimensional parameters relevant to this problem: (1) the classical Buckingham Pi Theorem and (2) considerations regarding the essential physical features of the problem.

The classical Buckingham Pi Theorem (Ref. 10) provides an algorithm for deducing a set of nondimensional parameters from a given set of dimensional parameters. Examination of the available reports on icing cloud testing yields the set of dimensional parameters listed in Table I. According to the Buckingham Pi Theorem, these 14 dimensional parameters, being comprised of the four fundamental dimensions, mass, length, time and temperature can be formed into 10 nondimensional groups. While this provides a comprehensive list of nondimensional parameters, it is likely that only a few of them are of first order importance for this study. Consequently, considerations regarding the essential physical features of the problem were employed to reduce the list of nondimensional parameters to those which are considered to be of dominating importance for the range of conditions of practical interest.

The overall shape of the cloud can be expected to depend on the retarding effect (drag) of the array, the array diameter and the mass and momentum flows of the injected water and air. The rate at which the injected fluid mixes with the surrounding air depends on the turbulent entrainment factor, α . Thus the longitudinal and radial flow velocities can be expressed in nondimensional form as

$$\frac{u}{u_{\infty}} = f \left(\frac{x}{R_0}, \frac{r}{R_0}, C_D, \alpha, \frac{\dot{m}_{air}}{\rho u_{\infty} R_0^2}, \frac{\dot{m}_w}{\rho u_{\infty} R_0^2}, \frac{u_{air}}{u_{\infty}}, \frac{u_w}{u_{\infty}} \right)$$
$$\frac{v}{u_{\infty}} = g \left(\frac{x}{R_0}, \frac{r}{R_0}, C_D, \alpha, \frac{\dot{m}_{air}}{\rho u_{\infty} R_0^2}, \frac{\dot{m}_w}{\rho u_{\infty} R_0^2}, \frac{u_{air}}{u_{\infty}}, \frac{u_w}{u_{\infty}} \right)$$

In addition, the properties of the droplets at a point in the cloud may be characterized by the droplet size distribution at the exit of the spray nozzles, the relative humidity of the atmosphere, the temperatures of the ambient atmosphere, injected liquid and injected air and the ambient pressure. Thus

$$\frac{LWC}{\rho} = h\left(\frac{x}{R_0}, \frac{r}{R_0}, \frac{r_d}{R_0}, \text{relative humidity}, \frac{T_w}{T_\infty}, \frac{T_{air}}{T_\infty}, \frac{p_w}{p_{sat}}, Re\right)$$

$$\frac{MVD}{r_d} = k\left(\frac{x}{R_0}, \frac{r}{R_0}, \frac{r_d}{R_0}, \text{relative humidity}, \frac{T_w}{T_\infty}, \frac{T_{air}}{T_\infty}, \frac{p_w}{p_{sat}}, Re\right)$$

Here Re is the Reynolds number based on the initial characteristic droplet radius, r_d , and the initial relative speed between the droplets and the air-stream. Note that the problem of droplet breakup in and immediately downstream of the nozzle exit, while an important factor in this problem, is beyond the scope of this project.

It can be seen from these functional relationships that the characterization of the droplet properties depends on the twelve nondimensional parameters

$$C_D, \alpha, \frac{\dot{m}_{air}}{\rho_{air} R_0^2}, \frac{\dot{m}_w}{\rho_w R_0^2}, \frac{U_{air}}{U_\infty}, \frac{U_w}{U_\infty}, \frac{r_d}{R_0}, \text{relative humidity}, \frac{T_w}{T_\infty}, \frac{T_{air}}{T_\infty}, \frac{p_w}{p_{sat}}, Re$$

The entrainment coefficient, α , is not likely to vary greatly over the range of conditions of interest. The drag coefficient may vary significantly from one configuration to another and must be included whenever comparing results using different arrays. It must be expected that the other parameters would play a significant role in any attempt to correlate the existing experimental data.

If data were available from existing experiments to evaluate these nondimensional parameters, one would expect that correlations of all such data could be obtained. Unfortunately none of the available reports were found to

contain enough information to permit evaluation any more than just a few of these parameters. Hence, no sensible correlation could be attempted. However, it seems likely that most of the information needed to calculate these parameters were available to the investigators but were not included in the reports. It is strongly recommended that reports on future experimental work include sufficient information to calculate these parameters.

There may understandably be some concern regarding the possibility of obtaining a useful correlation of experimental data from such a large set of parameters. It should be noted that the work reported in other sections of this report has established relations between certain of these parameters. Further work will certainly uncover additional relationships. These nondimensional parameters are in fact the key to combining future experimental and theoretical work into a useful design tool for icing studies.

REFERENCES

1. Shapiro, A.H., Wadleigh, K.R., Gavril, B.D., and Fowle, A.A., Transactions of the American Society of Mechanical Engineers, Vol. 78, pp. 617-653, 1956.
2. Hoffman, J.D., "An Analysis of the Effects of Gas-Particle Mixtures on the Performance of Rocket Nozzles", Ph.D. Thesis, Purdue University, Jan. 1963.
3. Willbanks, C.E. and Schulz, R.J., "Analytical Study of Icing Simulation for Turbine Engines in Altitude Test Cells". Arnold Engineering Development Center Report AECD-TR-73-144, Nov. 1973.
4. Miller, Charles M., "Numerical Method for Liquid Water Content Prediction in the Air Force Flight Test Center Icing Spray Cloud", Presented at the 6th Annual Symposium, Proceedings of the Society of Flight Test Engineers, Aug. 1975.
5. Schlichting, H., "Boundary Layer Theory", McGraw-Hill Book Co., 1979.
6. Epstein, M., "DESALE - 5: A Comprehensive Scheduled Mixing Model for CW Chemical Lasers", Aerospace Corpt. Dept. SAMS0-TR-79-31, May 1979.
7. Keenan, J.H. and Keyes, F.G., "Thermodynamic Properties of Steam", John Wiley and Sons, Inc., N.Y., 1961.
8. Pelton, J.M. and Willbanks, C.E., "A Kinetic Model for Two-Phase Flow in High Temperature Exhaust Gas Coolers", AEPC-TR-72-89, June 1972.
9. Dorsey, N.E., "Properties of Ordinary Water Substance", American Chemical Society Monograph, Series 81, Reinhold Publishing Co., N.Y., 1940.
10. Olson, R.M., "Essentials of Engineering Fluid Mechanics", Harper & Row, N.Y., 1980.

TABLE I

DIMENSIONAL PARAMETERS

Symbol	Description	Measured	Calculated
C_p	heat capacity		x
D	drag force		x
g	body force per unit mass		x
k	thermal conductivity		x
L	length	x	
\dot{m}	mass flowrate		
Q	volumetric flowrate	x	
p	pressure	x	
T	temperature	x	
u	velocity	x	x
β	thermal expansion		x
μ	viscosity		x
ρ	density		x
σ	surface tension		x

Note: Length may be drop diameter (d) or initial wake radius (R_o).
 Velocities may include freestream velocity (U) or local
 velocity components—i.e. horizontal (u_h) and radial (u_r).
 Other subscripts may include ()_a for injected air and ()_w
 for injected water quantities.

TABLE I (cont'd)

DIMENSIONLESS GROUPS RESULTING FROM BUCKINGHAM-PI ANALYSIS

Π_1	$= D / \rho u^2 \pi L^2$	$= C_D$	coefficient of drag
Π_2	$= \rho u L / \mu$	$= Re$	Reynolds Number
Π_3	$= p / \rho u^2 L^2$	$= Eu$	Euler Number
Π_4	$= u^2 / g L$	$= Fr$	Froude Number
Π_5	$= \mu C_p / k$	$= Pr$	Prandtl Number
Π_6	$= g \beta \rho^2 d^3 \Delta T / \mu^2$	$= Gr$	Grashof Number
Π_7	$= u^2 / C_p \Delta T$	$= Ec$	Eckert Number
Π_8	$= \rho u^2 / p$		dynamic over static pressure
Π_9	$= u \mu / \sigma$		surface forces
Π_{10}	$= Q \rho / \dot{m}$		mass flow ratio

DIMENSIONLESS GROUPS RESULTING FROM OBSERVATION

M	$= (\rho u)_w / \rho U$	momentum ratio (water / freestream)
R	$= R / R_0$	wake radius size
V	$= u_h / U$	horizontal local velocity
W	$= u_r / U$	radial local velocity
X	$= x / R_0$	distance from nozzle array
δ	$= d / L$	drop diameter ($L = R_0$ or MVD)
λ	$= LWC / \rho$	liquid water content
η	$= r / R$	local radius / wake radius

Note: $R_0 = R(@ x = 0)$ initial wake radius

LWC is liquid water content

MVD is mean volumetric diameter

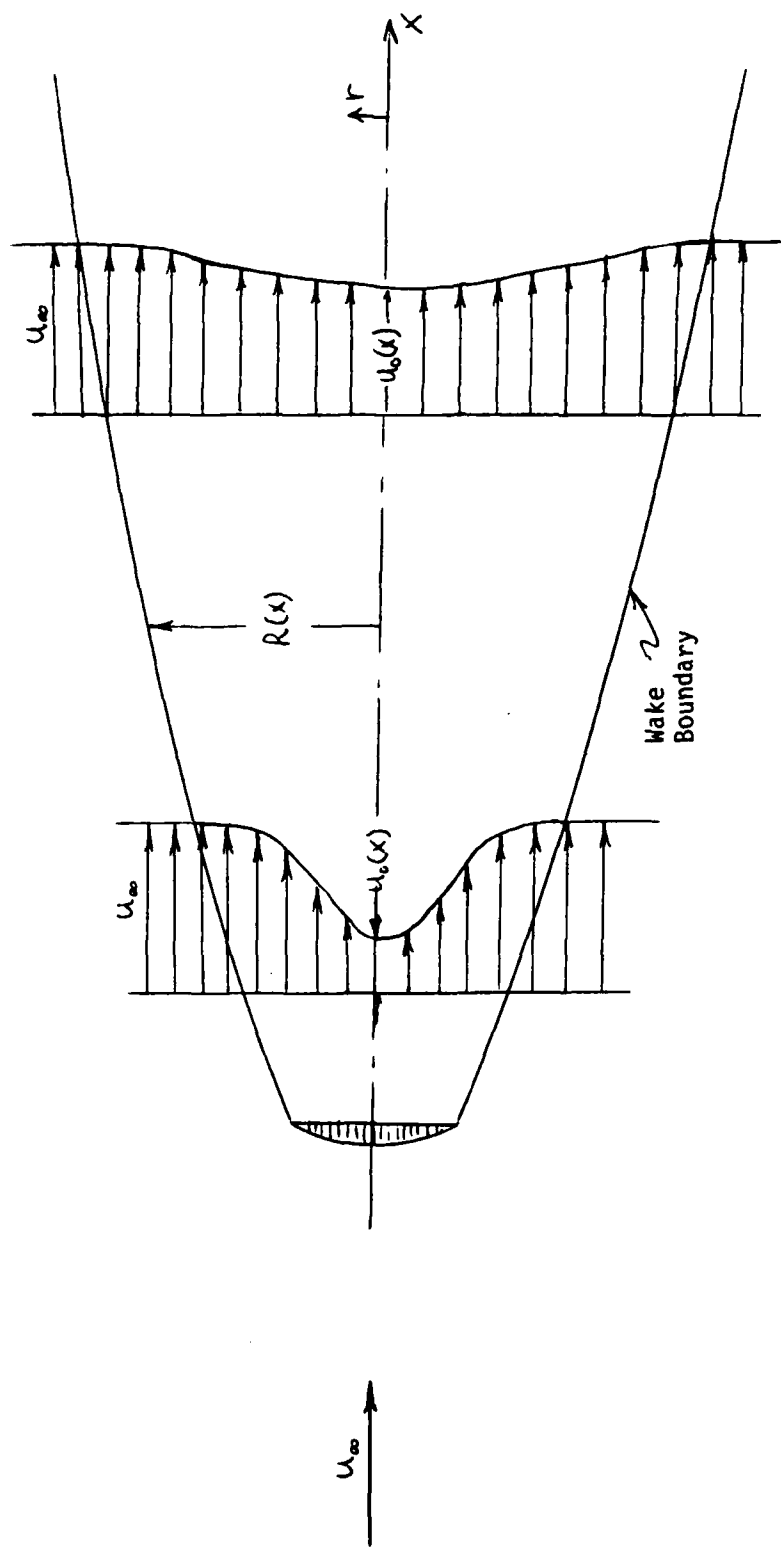


Figure 1 - Wake/Cloud Geometry

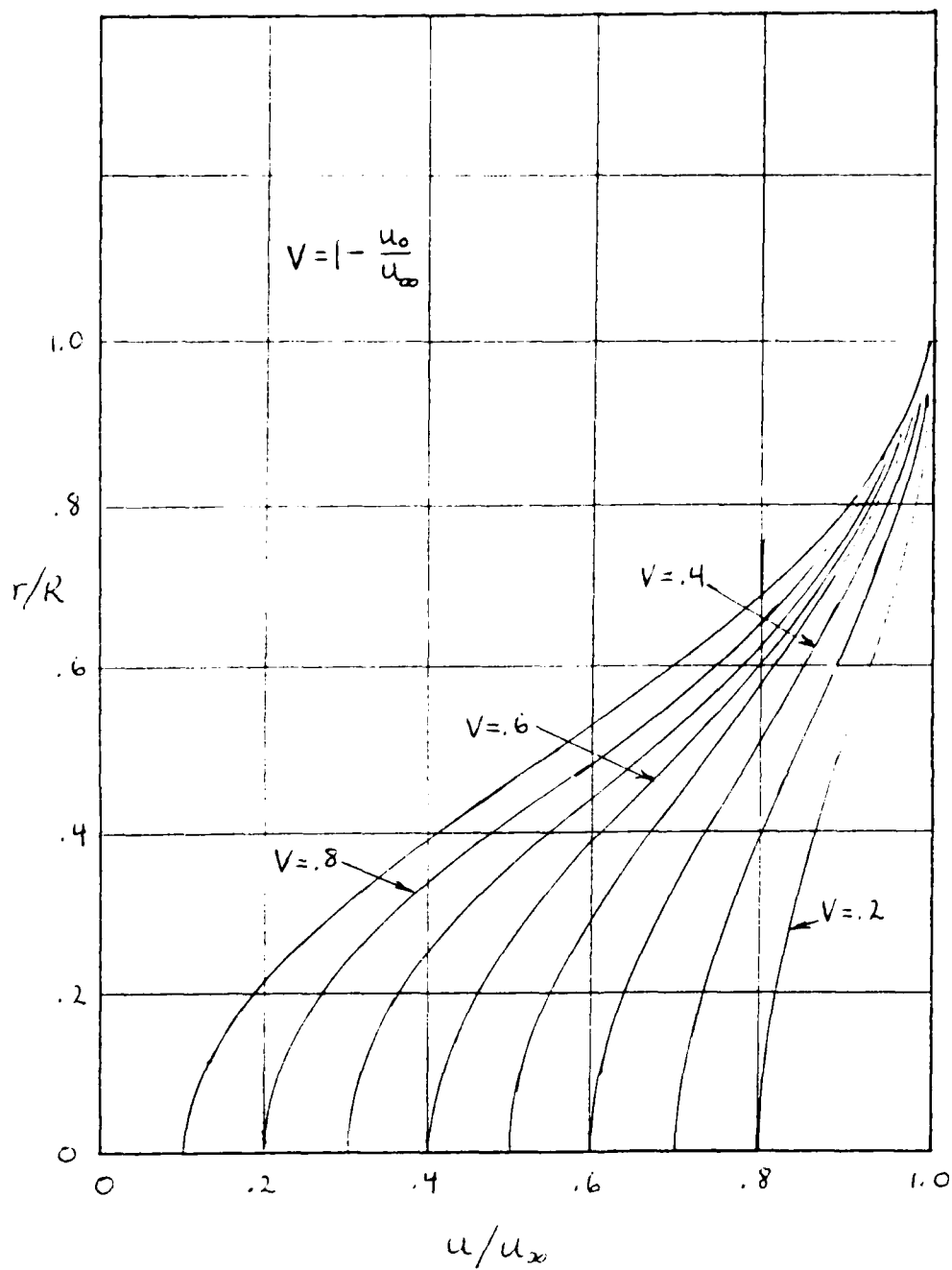


Figure 2 - Axial Velocity Profile

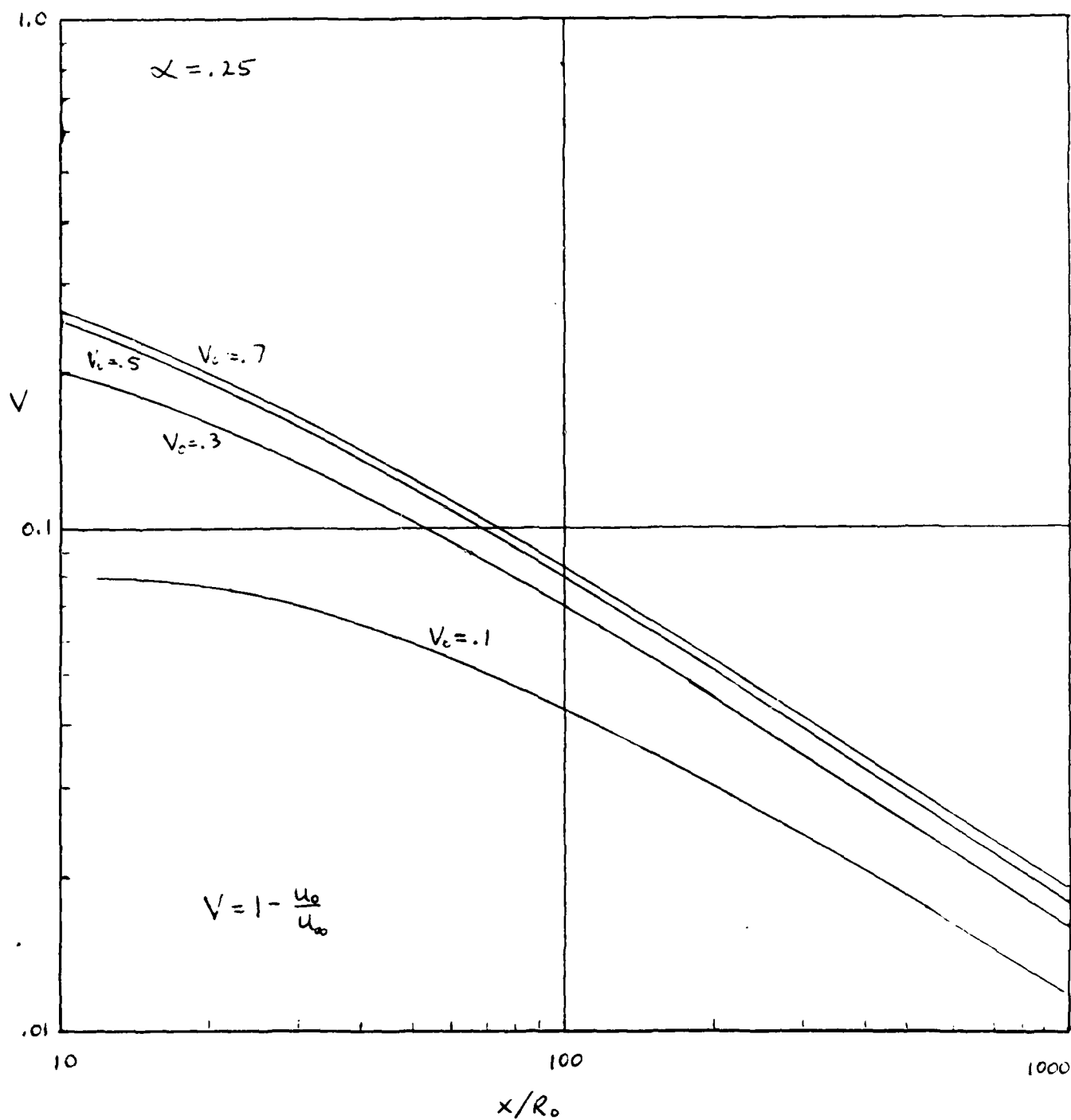


Figure 3 - Variation Of Axial Velocity Defect With Axial Distance

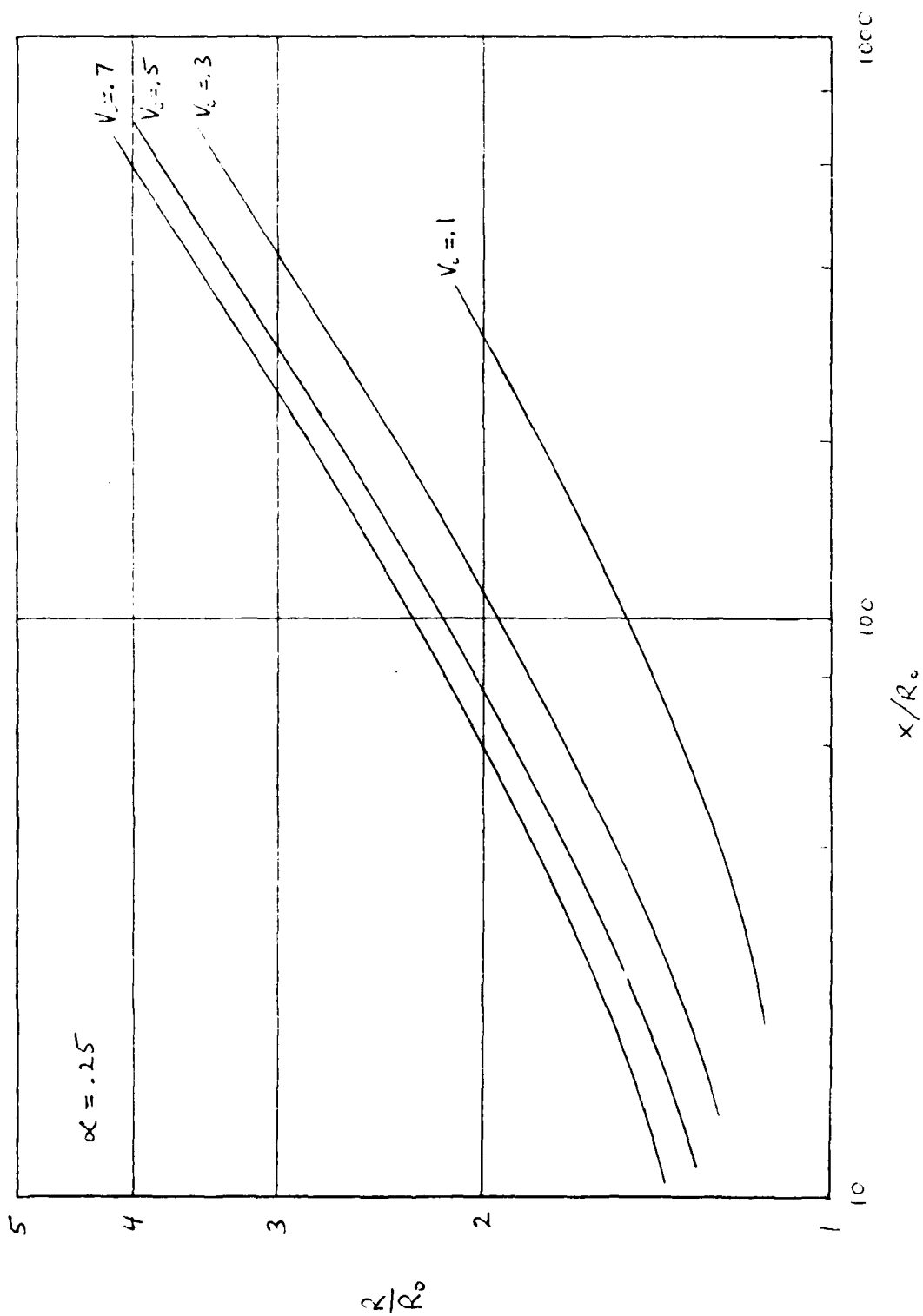


Figure 4 - Variation of Cloud Radius With Axial Distance

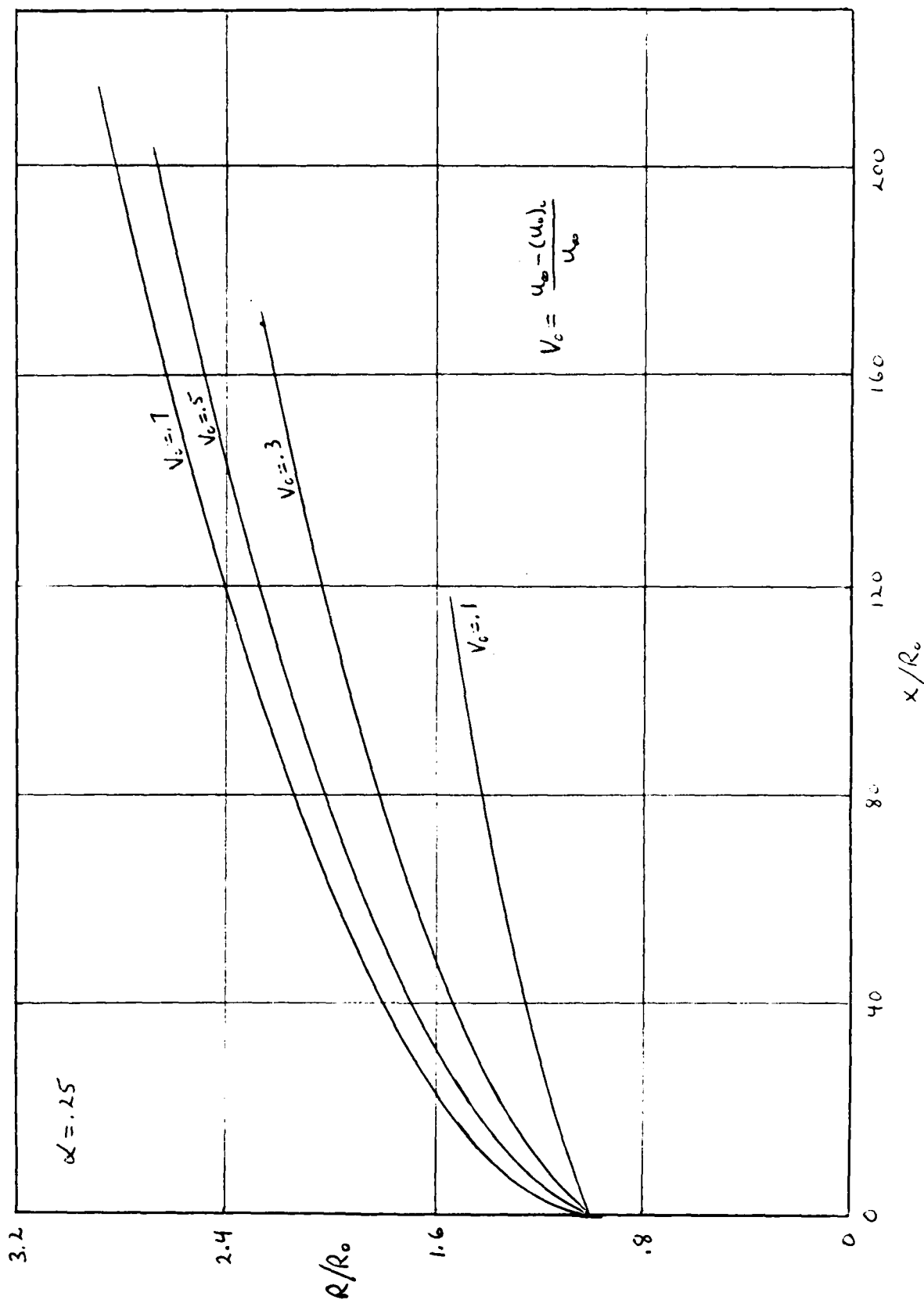


Figure 5 - Variation Of Cloud Radius With Axial Distance

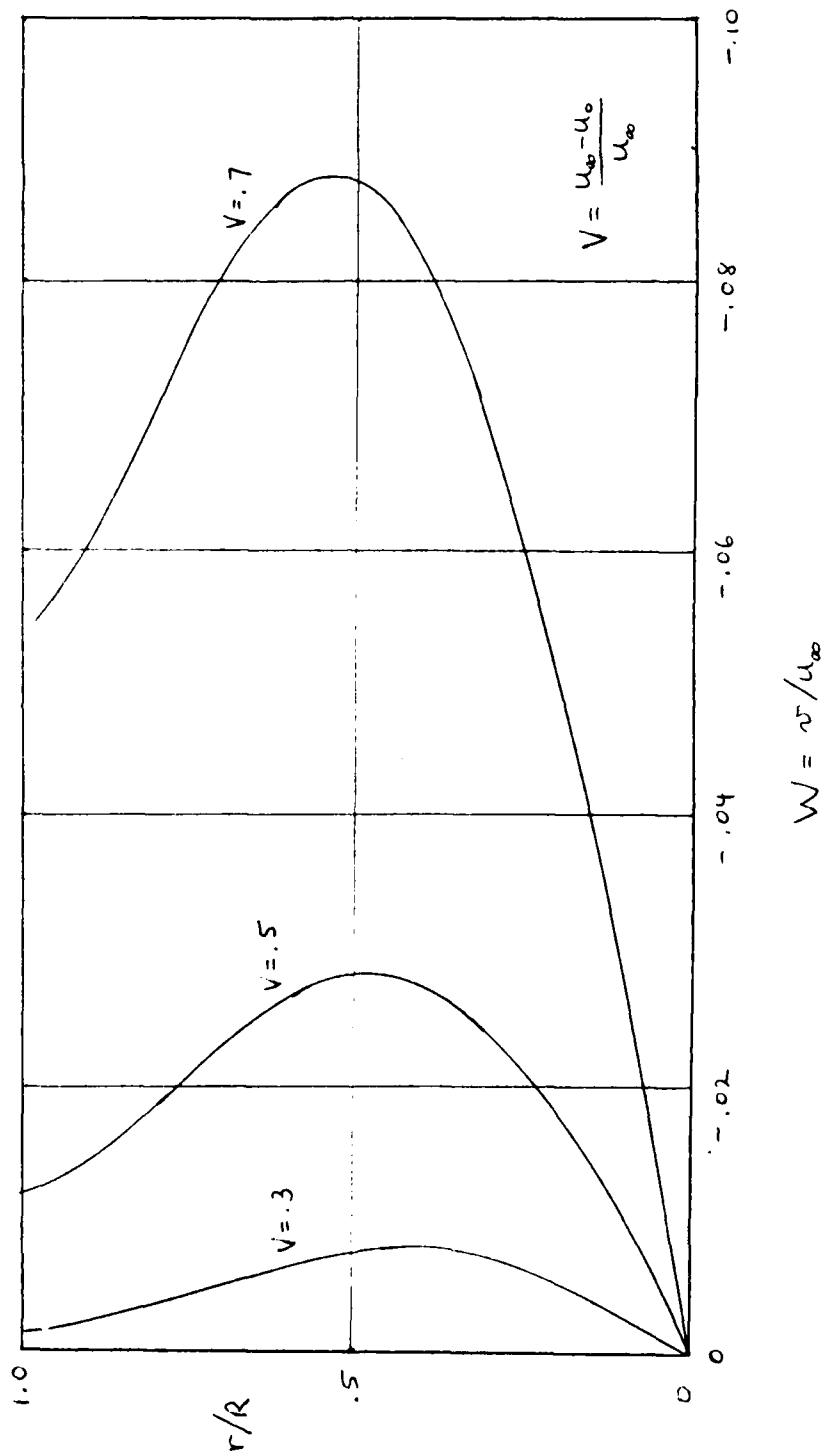


Figure 6 - Radial Velocity Profile

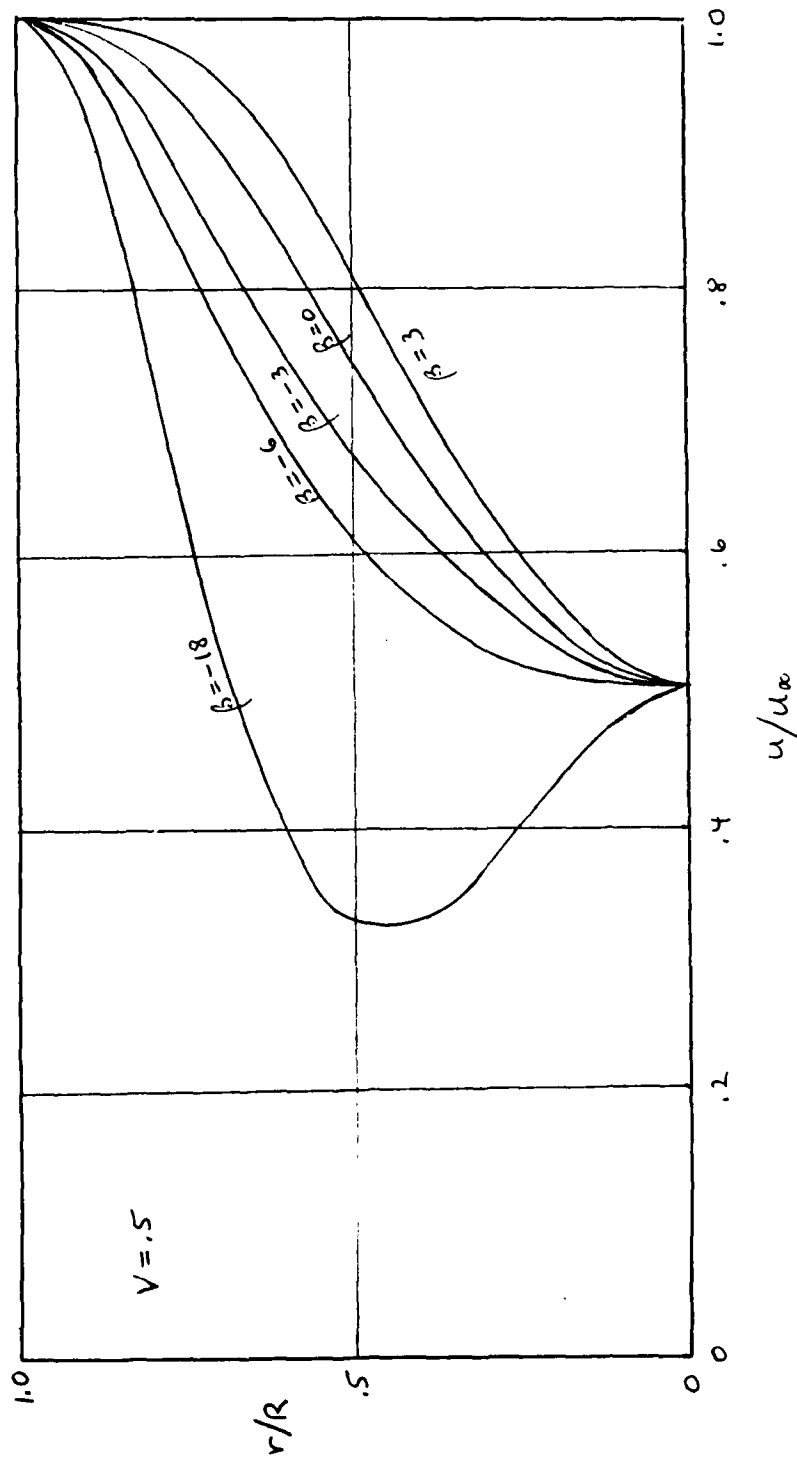


Figure 7 - Velocity Profile For Seventh Degree Polynomial

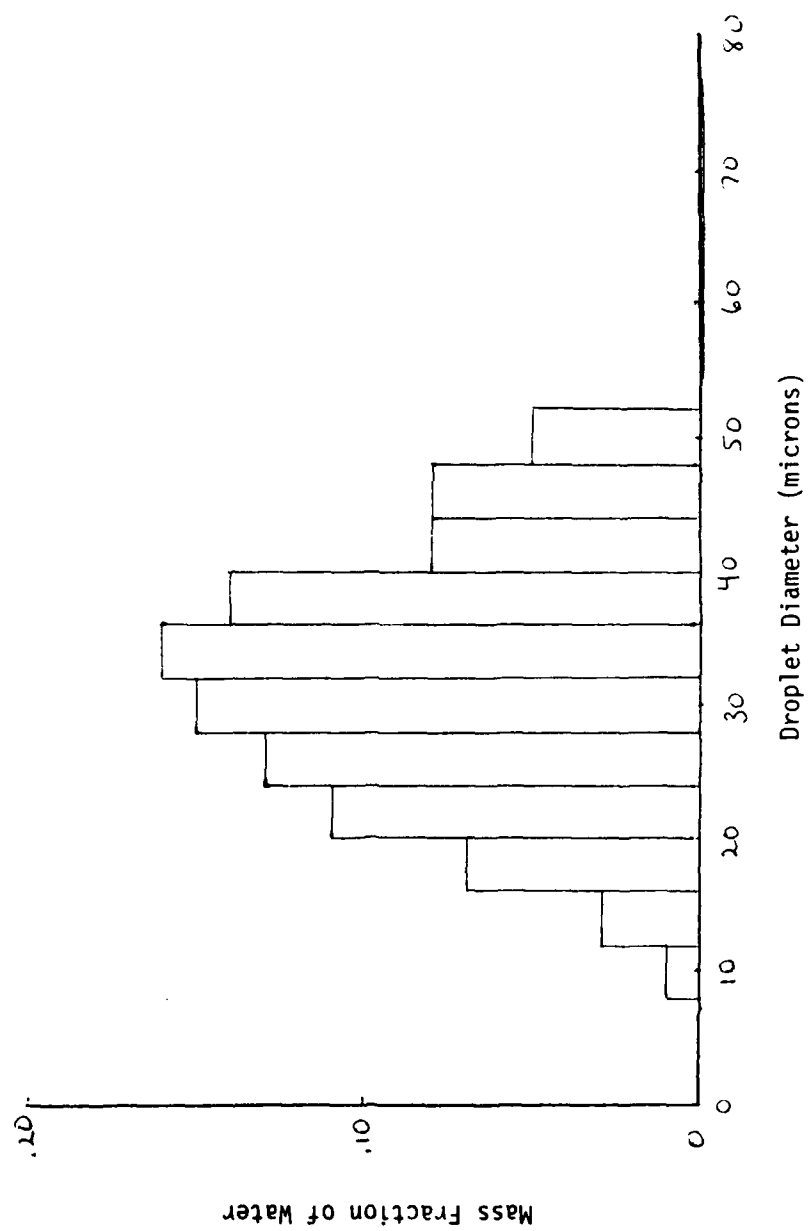


Figure 8 - Droplet Size Distribution (Ref.3)

DATE
FILMED
— 8